

# Connect-while-in-range: modelling the impact of spatial constraints on dynamic communication network structures

Niek Kerssies<sup>\*1,2</sup>, Jose Segovia-Martin<sup>1,3</sup>, James Winters<sup>4</sup>

**1** School of Collective Intelligence, University Mohammed VI Polytechnic, Rabat, Morocco

**2** Department of Sociology, Rijksuniversiteit Groningen, Groningen, The Netherlands

**3** Complex Systems Institute of Paris Ile-de-France, Centre national de la recherche scientifique, Paris, France

**4** Centre for Culture and Evolution, Department of Psychology, College of Health, Medicine and Life Sciences, Brunel University London, London

\*niek.kerssies@um6p.ma

## 1 Abstract

Like other social animals and biological systems, human groups constantly exchange information. Network models provide a way of quantifying this process by representing the pathways of information propagation between individuals. Existing approaches to studying these networks largely hypothesize network formation to be a result of cognitive biases and choices about who to connect to. Observational data suggests, however, that physical proximity plays a major role in shaping the formation of communication networks in human groups. Here we report results from a series of agent-based simulations in which agents move around at random in a bounded 2D space and connect while within communication range. Comparing the results to a non-spatial model, we show how including spatial constraints impacts our predictions of network structure: ranged networks are more clustered, with slightly higher degree, higher average shortest path length, a lower number of connected components and a higher small-world index. We

find two important drivers of network structure in range-constrained dynamic networks: communication range relative to environment size, and population density. These results show that neglecting spatial constraints in models of network formation makes a difference for predicted network structures. Our simulation model quantifies this part of the process of network formation, realized by simply situating individuals in an environment. The model also provides a tool to include spatial constraints in other models of human communication, as well as dynamic models of network formation more generally.

## 2 Introduction

Observational data suggests that physical proximity plays a major role in shaping the formation of social and communication networks in human groups [1, 2, 3]. Current experiments and models in human groups, however, focus mostly on static network structures chosen as conditions by researchers [4, 5, 6, 7, 8, 9, 10, 11, 12]. When dynamic networks are considered, network evolution is hypothesized to be shaped by individual connection biases, strategies or preferences [13, 14, 15]. Relatedly, models, experiments and fieldwork in cultural evolution have postulated "model-based" biases and strategies with which humans and other animals select others to observe, communicate and interact with [16, 17, 18, 19, 20].

For cognitive hypotheses on individual choices and biases like these to explain network formation, a simple condition needs to hold: each individual needs to be able to choose from the whole population under consideration at every point in time. In many natural settings, this condition does not obtain. To name just a few examples of network 'pre-selection', humans and other animals inherit social contacts from their parents [21, 22, 23, 24]; those with access to university education have access to many more social contacts [25]; and parental income and status impact properties of offspring social networks such as diversity of contacts [26, 27]. Social and communication networks are not shaped by individual choice alone, but prefigured partially by social as well as physical circumstances.

Physical proximity is a circumstance that is both very simple and very fundamental. Communication is an activity that takes place in an environment and using a physical communication medium with a functional range. Nonhuman animals employ various media such as chemical, visual, tactile, and seismic signals, while humans additionally use technologies ranging from conversations to the Internet [28, 29, 30]. Data from digital communications technology has greatly expanded our understanding of human communication networks [31, 32, 33]. However, many interactions remain face-to-face, as they have throughout much of human (evolutionary) history and in other social species. In these settings, physical proximity and location in the environment continue to play a much larger role. Moreover, the structure of online social networks is still shaped significantly by geography and existing real-world social ties [30, 31, 33]. Whether the group in question is a school of fish, a robot swarm, or a human crowd, part of the collective computation of communication network structure is not performed by individual decisions, but by the physical constraints of the environment and ranged communication.

In this paper, results are reported from a series of agent-based simulations designed to capture and quantify this dynamic. Agents randomly move through a 2D coordinate space and connect to others only while within a specified communication range. The resulting network structures are compared to results from a model without positions and movement in which agents connect at random. Like a recent model by Chimento and Farine [34], the model simulates the impact of movement through a 2D space on network structure and information transmission. Also like that model, we consider statistics of dynamic networks at each timestep, rather than properties of cumulative interaction graphs (static networks composed of interactions combined over time). Unlike that model, in which population size and communication range stay constant, we consider the complete meaningful parameter space of communication range and population density, mapping the influence of these parameters on 6 network structure measures, from  $N$  disconnected components to fully connected networks. Our model is also like a cellular automata model by Vining and colleagues [35] where agents move randomly through a 2D space and connect within range, though they focus on the impact of spatial constraints

on performance on a consensus task, rather than network structure outputs.

We find that introducing location, random movement and ranged communication introduces much more clustered networks, with slightly higher degree, higher average shortest path length, a lower number of connected components and a higher small-world index than a dynamic non-spatial model. All of these differences are more extreme when range is low. Our model shows how simply locating communicating individuals in an environment changes our predictions of the communication network structures that can form, and provides a tool for including spatial constraints in models of (communication) network formation. In so doing, the model also functions as an agent-based alternative to existing network formation algorithms, creating networks from bottom-up interactions between nodes rather than setting top-down global node properties.

### 3 Materials and methods

#### 3.1 Model

##### 3.1.1 Random movement and the range rule.

In agent-based models, each of a population of agents follows an update rule every timestep. In this model, the model parameters are  $N$ ,  $g$  and  $r$ .  $N$  is the population size,  $g$  is the grid size such that  $g * g$  is the area of the coordinate space, and  $r$  is agent communication range.  $N$  agents are initialized and assigned a unique random coordinate value  $(x,y)$  within the  $g * g$  grid.

Each timestep, every agent (1) moves, (2) connects, and (3) disconnects. To move, an agent chooses from a uniformly random distribution of its adjacent integer coordinates, including its current location. In other words, it selects a tile at random in its Moore neighborhood. To keep agents within the bounded space and to prevent agents sharing the same position, tiles within the neighborhood with coordinate values below 0 or exceeding  $g$ , and tiles currently occupied by other agents, are excluded from the random selection of a new position. If all tiles in the neighborhood are out of bounds or occupied,

the agent remains in the current position.

To connect, after moving, each agent creates an undirected network link with all other agents that are currently in range. Range is calculated as Euclidean distance in the coordinate space, rounded to integer values for x and y. Euclidean distance uses the Pythagorean theorem that for right-angled triangles,  $c^2 = a^2 + b^2$  (where  $a$  and  $b$  are the base and altitude, and  $c$  the hypotenuse of the triangle). Agent  $i$  checks whether agent  $j$  is in range by putting the difference in coordinates  $x_j - x_i$  and  $y_j - y_i$  as  $a$  and  $b$ , and calculating the distance to  $j$  as  $c$ ; so  $r = \sqrt{(x_j - x_i)^2 + (y_j - y_i)^2}$ . If the result is less than or equal to the value of  $r$ , agent  $j$  is within range. Finally, to disconnect, the agent deletes any links with agents that are no longer in range. The order in which agents are updated is randomized each timestep. Fig. 1 shows the initialization and first timestep of a possible model run schematically.

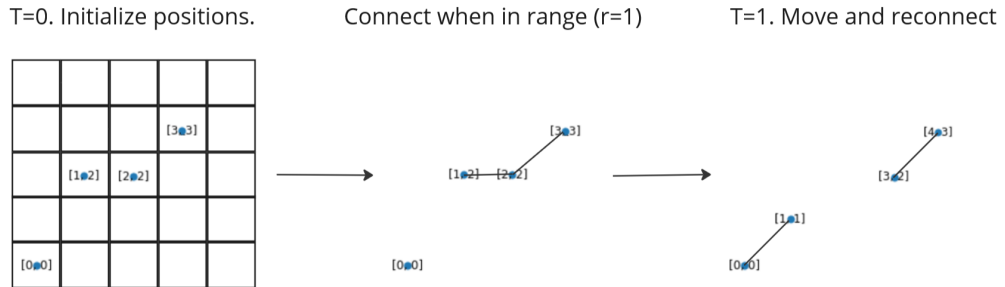


**Fig 1. Demonstration of a possible initialization and timestep in the model for  $N = 4, r = 1, g = 4$ .** Agents are randomly assigned a unique (x,y) coordinate. The coordinate space is graphically represented here as a grid(left), and agents are shown with their coordinate values. At every timestep, every agents follows the range rule: if the Euclidean distance between the agents is less than or equal to  $r$ , a link is created between them. Thus, from the initial position shown on the grid, the graph shown in the middle of the figure is formed. At the start of the next timestep, agents move at random and follow the range rule again. When previously in range agents are now out of range, the link is cut. Hence, from every agent performing random movement and following the range rule, a new network is formed.

### 3.1.2 Null model.

The intention of the simulations reported in this paper is to demonstrate the work being done by spatial constraints on communication network formation. In order to do so, the results are compared to a non-spatial model. In the non-spatial model, each timestep agents simply connect to each other agent with probability  $P(connect)$  which is set globally as the same for all agents. In order to compare this model's outputs to that of the

range model,  $N$  can be set to the same value or varied in the same range of values, while  $P(\text{connect})$  corresponds to  $r$ . Like  $r$ , the  $P(\text{connect})$  parameter can be varied through its whole meaningful range of values, from isolated agents to fully connected networks. A connection probability of 0 will mean  $N$  unconnected nodes, while a probability of 1 will always create fully connected networks. The parameter  $g$  has no equivalent in the non-spatial model and there are no coordinates assigned to agents. Finally, in order to make the non-spatial model a dynamic process as well, a random disconnect chance is included, which is set to  $1 - P(\text{connect})$ . This way, the probabilities of connecting and disconnecting mirror those of the range model, as the area not covered by an agent's range is equal to the inverse of the area covered (for a calculation of connection probability under random movement and ranged communication in an unbounded space, see [35]).

### 3.2 Test setup

Simulations consisted of several tests. In a test, one of the model's three input parameters  $N, g, r$  was chosen to vary while the others remained constant. For each integer value of the varying input parameter, both the range and the null model ran for 100 rounds of 100 timesteps, where at each timestep, all agents were updated in a random order and output measures were collected.

For the first set of tests, range was varied between  $r=0$  and  $r = 10$  while  $N$  was kept at constant values, varying between tests from  $N = 1$  to  $N = 100$  (see Fig. 2 for results for  $N = 20, 40, 60,$  and  $80$ ). Varying range up to  $r = g$  ensures that in terms of network structure, the complete meaningful range of  $r$ -values is tested. At  $r = 0$ , no nodes are connected; at  $r = g$ , where the diameter of each agent's range covers the whole length of the coordinate grid, networks are always fully connected. In the null model, the connection probability parameter  $P(\text{connect})$  was varied between 0 and 1 with intervals of 0.1, similarly ensuring that the simulations start at disconnected nodes and end at fully connected networks.

In the second set of tests, in each test  $N$  in both the range and the null model was

varied between 1 and 49, while  $g = 7$  and  $r$  varied at constant values between tests, from 0 to 7.  $N$  varies up to 49 because when  $g = 7$  there are  $7 * 7 = 49$  unique positions in the environment. Since agents avoid sharing the same position, as  $N$  increases towards  $gxg$ , the space becomes increasingly "crowded" until it is completely saturated and agents remain in place, each in a unique position. For this parameter, then, the meaningful range is determined by population density  $N/(g * g)$ , varying between  $1/49$  at  $N = 1$  and  $49/49 = 1$  at  $N = 49$ . Since it lacks spatial positions, the null model has no analog to  $g$ . Therefore we show results here only for varying  $N$ ; for varying  $g$ , see the supplemental materials. In the null model,  $N$  was varied over the same values while  $P(connect)$  was set to  $r/g$ . This way the null model mimics the connection probability of the range model, in which an agent's probability to connect is proportional to the range relative to the environment size.

### 3.3 Output measures

Each timestep, 6 network properties were calculated in both models. The network properties calculated are average degree, clustering coefficient, average shortest path length, number of connected components, size of largest component, and small-world index.

Networks (sometimes called graphs) are mathematical objects represented by dots (nodes or vertices ) and lines (links or edges) between the dots. Degree is a property of single nodes: the amount of connections it has in the network. The average degree  $K$  is simply the population average of node degrees  $k_i$ :  $K = \frac{\sum_{i=1}^N k_i}{N}$ . In this model, nodes do not connect to themselves and redundant connections are not possible. Therefore, the maximum amount of connections one node can have is  $N - 1$ . For a population of 10 nodes, average degree will therefore be a value between 0 and 9. Note that if the population average degree is equal to  $N - 1$ , this indicates a complete graph: the network where each node is connected to all other nodes.

Clustering indicates the fraction of a node's network neighbors that are themselves connected to each other. To illustrate, say node A is connected to three others B, C and

D. B and C are connected, but C and D are not and neither are B and D. In this case, ABC forms a fully connected triangle, while ABD and ACD do not. Clustering can be indicated as the ratio of actual to possible fully connected triangles, in this case  $1/3$ . This is the clustering coefficient. This coefficient is calculated for the whole network each timestep, resulting each time in a value between 0 and 1. Note that a value of 1 for this coefficient corresponds to the complete graph at which average degree is  $N - 1$ ; if all possible triangles are fully connected, then the whole network is fully connected.

The shortest path length between two nodes is amount of links that need to be traversed in order to get from one agent to the other. Average path length is the average taken over all node pairs. Here, too, an average value of 1 means that the networks are fully connected, since it indicates that all pairs have a direct path of 1 link between them.

In this model, the agents will not always form a single network. More often, especially at low range (and at low connection probability in the null model), the population will consist of several mutually unconnected local networks, or single isolated nodes. We calculated the number of such connected components and the size of the largest connected component. When the number of components is 1, the population forms a single connected graph; when it is equal to  $N$ , no nodes are connected. Conversely, when the largest component is equal to  $N$ , the population forms a single connected graph, and when it is 1, no nodes are connected. Note that a population that forms a single connected network, where there is at least one path between all nodes, is not necessarily a fully connected network, where there is a direct link between all nodes.

Finally, we calculated the small-world-index of networks. Strictly speaking, a small world network is one defined by the parameters  $n, k$  and  $p$ , where  $n$  is the population size,  $k$  is the number of neighbors on a ring lattice that each node connects to (therefore each node has the same degree  $k$ ), and  $p$  is the probability that a link is "rewired": replaced by a link to a node chosen at random from the whole population [36]. A direct comparison between a small-world networks and range model networks, however, does not make much sense, for two reasons. First, the range model is a spatial model: in a



small-world network, nodes have a fixed position on a ring lattice, while in the range model, nodes move around through a 2D coordinate space. Second, in a small-world network  $k$  specifies a global degree value. When rewiring probability  $p$  is 0, this means that all nodes have degree  $k$ . This is very rare in a dynamic, spatially explicit model with random movement; it can only occur when agents happen to form an equidistant ring in space.

In order to still have an indication of the occurrence frequency of small-world-like structures, there is the small-world index [37]. The small-world index  $S$  of a graph  $G$  is the ratio of  $C$  to  $L$ .  $C$  is equal to  $CG/CR$ , where  $CG$  is the clustering coefficient of  $G$ , and  $CR$  is the clustering coefficient of a random graph with the same number of  $n$  nodes and  $m$  edges as  $G$ . Similarly,  $L$  is equal to  $LG/LR$ , where  $L$  is the average shortest path length.  $S$ , then, is calculated as  $S = (CG/CR)/(LG/LR)$ . This measure captures the feature of small-world graphs that most nodes are locally connected, while some are rewired to form 'longer' ties outside of local clusters. Adding only a few of such long ties connects relatively clustered local communities, creating much shorter average shortest path lengths while keeping clustering high [36]. If, therefore, clustering is low and average shortest path length is high compared to a random model,  $S$  will be low; if the opposite is the case,  $S$  is high.

## 4 Results

### 4.1 Ranged communication creates much more clustered graphs than a non-spatial model.

The most conspicuous difference between the range model and the null model is the difference in clustering. At lower values of  $r$ , the average clustering coefficient of networks increases sharply with increasing  $r$ . The non-spatial model behaves in almost opposite fashion, networks with higher  $P(connect)$  showing an initially slow and eventually steeper increase in clustering.

Part of this difference in clustering is accounted for by the difference in average

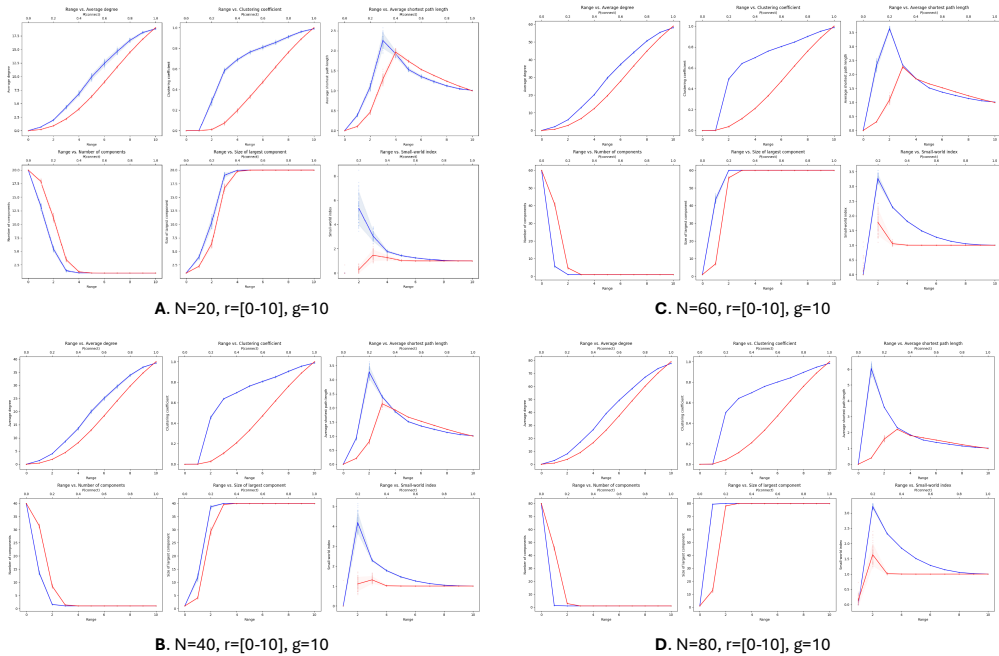


**Fig 2. Network properties of range model (blue) and null model (red) networks for varying range between 0 and 10 (x-axes) within runs and varying population density 0.2,0.4,0.6, and 0.8 between runs (top to bottom).** Dots in the graphs are time-averages of 100 timesteps, of which 100 rounds are collected at each input setting of  $r$ . Lines are drawn through the means of these time averages, and transparent areas show 1.5 standard deviations. Most visibly at low range settings (when spatial constraints are most articulated), networks are much more clustered, have slightly higher degree, higher average shortest path length, a lower number of connected components and a higher small-world index than the null model. As  $N$  varies between tests, most network measures stay the same, being predominantly influenced by  $r$  in the range model and  $P(\text{connect})$  in the null model. At lower range settings, however, average shortest path length (and as a result, small-world index) increases noticeably with increasing  $N$ , as the disconnected groups that form at lower range settings become larger while still being highly clustered.

degree. As communication range and connection probability increase, agents form more connections, leading to higher population average degree. As more of the possible connections between agents are made, more connected triangles form, increasing the clustering coefficient. In the non-spatial null model, this effect seems to account for the increase in clustering, which closely follows the increase in degree.

In the range model, however, this straightforward relationship between degree and clustering is not observed, especially at lower values of  $r$ . This is because there is an additional effect increasing clustering, introduced by range-constrained network formation. In the non-spatial model, the formation of closed triangles is purely a matter of chance: namely, the chance that an agent  $A$  at one timestep  $t$  is connected to both agent  $B$  and  $C$  (or has been at a timestep before  $t$ , and has not since disconnected),

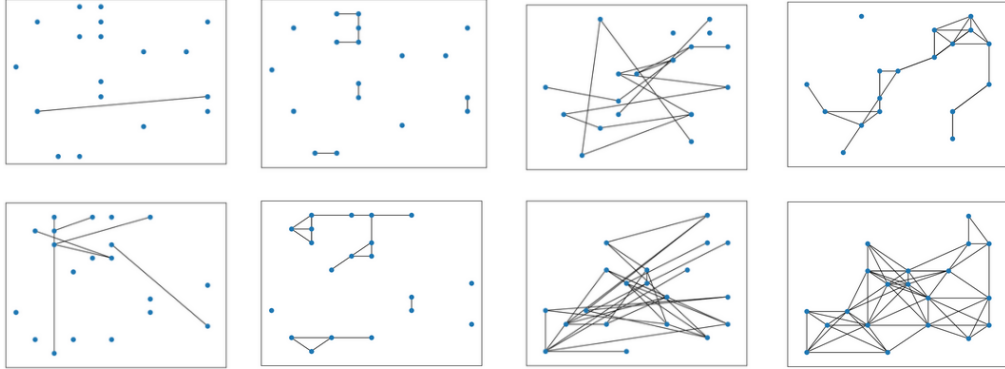


**Fig 3. Four sample network timesteps comparing the null model (left) to the range model (right),**  $N = 18, g = 10$ . Upper left:  $r = 1, pc = 0.1$ . Lower left:  $r = 2, pc = 0.2$ . Upper right:  $r = 3, pc = 0.3$ . Lower right:  $r = 4, pc = 0.4$ . The spatial layout created by the positions of the agents in the range model graphs are copied in the null model comparisons. At similar connection probabilities, agents in the range model only connect to closer agents, creating more connected triangles.

and that additionally B and C are connected at  $t$ . Hence, degree and clustering simply increase as this connection probability  $P(\text{connect})$  increases. In the range model, there is a condition of physical proximity to network links. Since movement is random, the probability of two agents A and B being within range and therefore connected is also well-modelled as a random process, where connection probability is proportional to the percentage of the area covered by an agent's range [35]. For any two connected agents A and B, B needs to be within the area covered by the communication range of agent A. For a third agent C, however, to connect to A, it needs to be within this area as well. For randomly moving agents, this means the space of possible coordinates drawn from in the random movement step is reduced from the entire space  $g * g$  to the agent range area  $2\pi r$ , which is significantly smaller when  $r : g$  is low. This means that if both B and C are connected to A, they have a much higher chance (than agents not connected to A) to connect to each other as well. Therefore, networks become more clustered simply because of introducing spatial communication constraints. As range increases, this requirement becomes less strict, as the likelihood that agent C in this example is close to agent B decreases as  $r$  tends to  $g$  and the area covered by a single agent's range increases proportionally. Fig. 3 illustrates this point with network visualizations.

This same effect accounts for a lower average shortest path length in the range model. In the null model, any node can connect to any other node, generally creating 'well-mixed'

networks with no preference for specific nodes. In the range model, there is a preference for connecting to agents close in the coordinate space, and as a result, a tendency to form local clusters. 'Long ties' that bridge these locally clustered communities are more rare and only happen on the edges of spatially clustered communities. As range increases, the clustering effect decreases while at the same time the formation of between-community ties becomes easier. This creates a distinct 2 phases to average shortest path length with increasing range. In the first phase, from  $r : g = 0$  to  $r : g = 0.2$ , networks have increasingly higher average shortest path length, as distinct clustered groups form. After  $r : g = 0.2$ , average shortest path lengths start to decrease, as the clustering effect diminishes and longer connections form between the groups, until fully connected networks are reached at  $r = g$  and average shortest path length becomes 1. These two phases are also reflected in the number of components; high in the first phase, quickly becoming a single component in the second. In the null model, a similar effect occurs, though average shortest path length stays generally lower because of the lack of a connection preference such as the clustering mechanism in the range model.

As a direct result of the large difference in clustering and average shortest path length, the range model networks have much higher small-world index when range is low. Introducing spatial constraints produces more 'small-world-like' networks, most notably so when  $r : g = 0.2$ .

## **4.2 Range constrains the influence of population density on network structure.**

For constant values of  $r$  and  $g$ , varying population size  $N$  also impacts network structures in the range model. In both the null model and the range model, as population size increases, so do average degree and the size of the largest connected component. In the null model, degree increases with  $N$  because as more nodes are added, there are more possible links, meaning more instances of checking  $P(connect)$  and therefore a higher probability of more connections per node. In both models, the size of the largest component simply increases with  $N$  since the total number of nodes is higher.

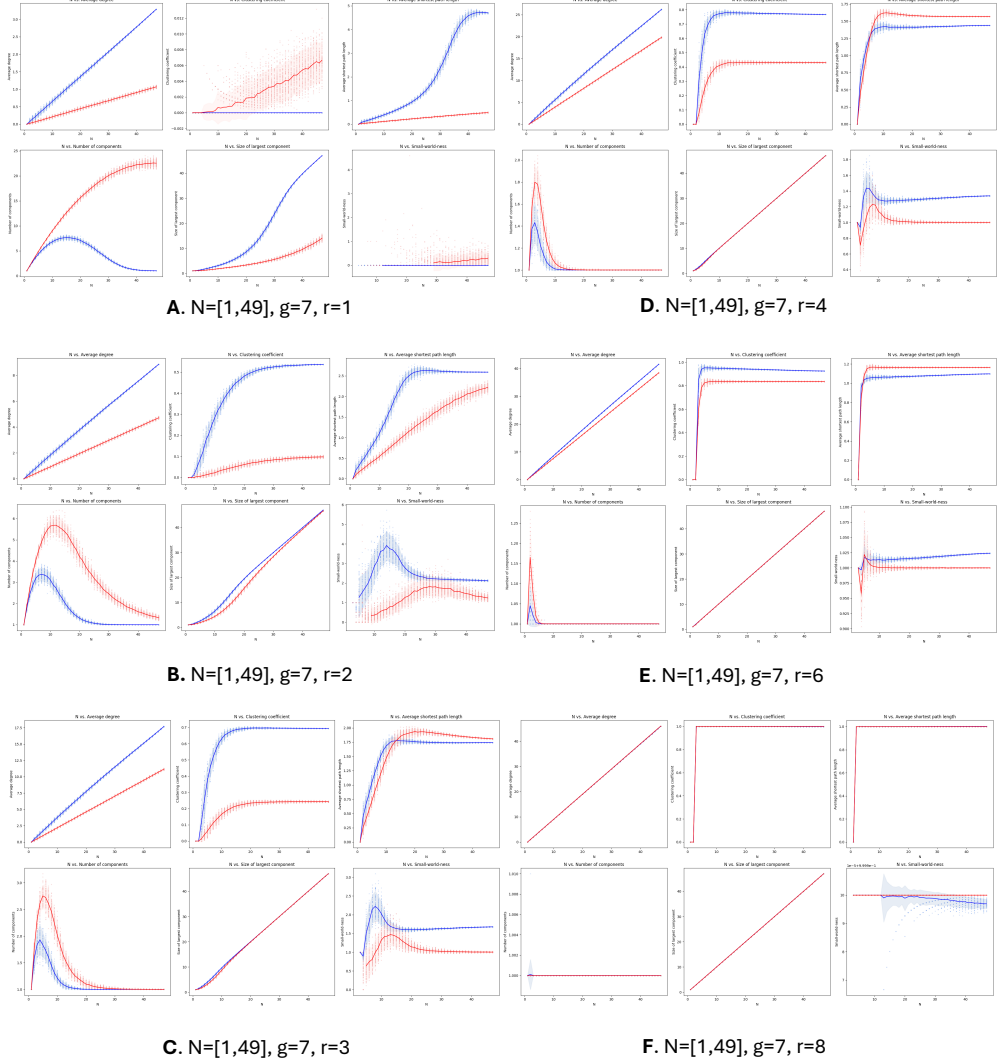


**Fig 4. Network properties of range model (blue) and null model (red) networks for varying  $N$  between 1 and 49 (x-axes) within runs and varying  $r$  1, 2, 3, 4, 6, 8 between runs. Dots in the graphs are time-averages of 100 timesteps, of which 100 rounds are collected at each input setting of  $r$ . Lines are drawn through the means of these time averages, and transparent areas show 1.5 standard deviations. Varying  $r$  has a clear impact on the relationship between population density and all 6 network measures, determining how densely connected graphs can become as  $N$  increases. When  $r$  approaches  $g$ , the role of agent locations diminishes until networks in the range model become like the non-spatial null model.**

In the null model, average shortest path length and number of components show a slightly more complex relationship with  $N$ . For static Erdos-Renyi random graphs, it has been shown that for each connection probability value there is a critical  $N$  at which a giant component is formed, including most or all nodes [38]. This dynamic version of the same random process shows a similar behavior. At lower values of  $N$ , the average number of connected components in null model networks increases steeply. After reaching this peak, the number of connected components decreases again, reaching 2 at  $N = g^2$ . Average shortest path length follows a similar two-step progression, initially increasing, reaching a brief plateau, and then increasing again until reaching 2 at  $N = g^2$ . These two measures describe the formation of a giant component as  $N$  increases. In the first phase of increasing  $N$ , the number of components increases, as the connection chance plus the number of nodes 'trying' to connect is not high enough to form more than isolated smaller components of 1 or 2 nodes. Average shortest path length increases to a value between 0, where no nodes are connected, and 1, while the number of components stays at close to  $N/2$ , indicating that mostly connected pairs form. As  $N$  increases further, nodes become more connected and the number of components starts to fall, tending towards a single component. Average shortest path length starts another slight increase because, while the network tends towards a single component, as more nodes are added, the network diameter (the longest shortest path in a network) of that component increases as well, increasing the probability that the distance between peripheral nodes and nodes at the opposite side of the component grows. Overall, however, average shortest path length stays low, reaching a maximum of 2, reflecting the ability of random graphs to mix well.

The range model echoes some of these dynamics, but adds others. In the range model, the increase in degree and average shortest path length with  $N$  is much steeper, and the number of connected component stays lower throughout. These additional effects of population size in the range model are due to agents being situated in a bounded space. As  $N$  increases while  $g$  remains constant (or when  $g$  decreases while  $N$  remains constant), population density  $N/gxg$  increases. With population density, the probability

of randomly moving agents being in range of each other increases, increasing the network density more than  $N$  otherwise would, as expressed by a higher average degree and a lower number of connected components than in the null model. Because agents avoid shared coordinates, as  $N$  increases they become both closer and more evenly spread out over the coordinate space, leading to single connected component for much lower values of  $N$  than is the case in the null model, where random connections can leave nodes isolated. The additional increase of average shortest path length with  $N$  is due to the effect of range-constrained communication described above, which leads to more clustered networks.

For varying  $N$  even more than for varying  $r$ , the range model shows much higher clustering than the null model. Unlike average shortest path length, number of connected components, size of largest component, and degree, there is little to no relation between  $N$  and clustering in the null model. Once again this is consistent with existing knowledge of static random graphs: As  $N$  increases, the number of possible edges grows, but the likelihood of any specific pair or triangle of nodes being connected remains governed by  $P(\text{connect})$  [39]. In the range model, by contrast, clustering increases with population density. As discussed above, the constraint on communication range tends to cluster nodes together. Additionally, graph density increases as population density increases, leading to an even bigger contrast with the null model.

Finally as  $N$  increases, clustering, average shortest path length, and number of connected components reach a "plateau", remaining at a constant value. These are limits imposed by the range parameter. As population density increases, clustering would increase further if  $r$  would not impose a limit on the possible connections that can be formed, and therefore on the number of connected triangles. Fig. 4 visualizes how for different values of the range parameter, clustering reaches the plateau at different values. The same is true for average shortest path length: when range approaches  $g$ , there are no restrictions on possible connections and the average shortest path length tends to 1, indicating a fully connected network. However, when range is lower, increasing  $N$  increases the average shortest path length as population density increases the graph

density while the network remains relatively clustered. As range decreases, the maximum average shortest path length reached increases. Note that this limit is also visible in the results for average degree. As explained above, a fully connected network has an average degree of  $N - 1$ . In contrast to that, see for example Fig.4B: for  $N = 20$ , maximum degree would be 19, but the results show an average degree of 3.9. Similarly low scores are shown throughout, degree staying far from the possible maximum. This, too, is due to range. Average degree does increase as more agents occupy the coordinate space, but because connections are limited to agents in range, the extent to which it increases is limited as well. As this limiting factor of range decreases as range approaches  $g$ , the null and range models start to resemble each other more (see Fig. 4).

To summarize the simulation results, we found two major network formation mechanisms introduced by a coordinate space, random movement, and ranged communication. First, for any constant population size, the ratio of  $r$  to  $g$  determines how densely connected graphs are, from disconnected nodes at  $r = 0$  to fully connected networks when  $r > g$ . Second, independently from communication range, increasing the population density  $N/g^2$  also increases graph density, as agents 'crowd' the coordinate space, making connections more likely, until they each occupy one of the possible coordinates when  $N = g^2$ . The impact of increasing population density on graph structures is still determined by  $r$ , each node relying on movement for connection when population density is low, but reaching the maximum degree and clustering possible under the current value of  $r$  when the population density reaches 1. Range (relative to coordinate space size  $g$ ) therefore sets the slope of the increase of graph density with population density, as well as 'plateau' maximum values to the increase in clustering, decrease in average shortest path length, and decrease in number of connected components.

In addition to tracking network properties outputs, our simulations included four commonly modelled processes of information diffusion on the networks. These simulations reproduce known results on network properties and information diffusion [5, 11, 36, 40]. For example, when range is low and therefore the number of connected components and clustering are high, information spreads more slowly, and the population explores more



complex problem spaces more effectively than the null model. These results illustrate how spatial constraints impact not just our predictions of communication networks, but also (and as a result) our predictions of transmission processes that take place on these networks. For details, see the supplemental materials.

## 5 Discussion

In this paper, we report simulations demonstrating that including spatial constraints on communication introduces significant differences in network architectures (and by extension in information flow: see supplemental materials). In general but especially when range is low compared to environment size  $g$ , networks are more clustered, have higher average shortest path length, a lower number of connected components, and a higher small-world index than dynamic random graphs. Two main parameters drive average network structures: communication range  $r$ , relative to  $g$ , and population density  $N/g^2$ . As either increases while the other remains constant, graphs become more densely connected. The influence of population density on graph density is bounded by  $r$ , limiting the possible connections agents can make. As population density increases, movement becomes increasingly impossible as every agent occupies one of the  $g * g$  coordinates when  $N = g^2$ . As a result, positions become fixed and node properties become global, set by the value of  $r$ . A specific mechanism that causes higher clustering and average shortest path lengths in ranged networks is that any agents  $j$  connecting to an agent  $i$  need to be within the area covered by  $i$ 's range, significantly increasing the probability that agents  $j$  connect to each other as well. We also show that range-constrained networks create more small-world like networks.

One obvious but central result of our simulations is that when communication range  $r$  exceeds grid size  $g$ , fully connected communication networks are guaranteed. In other words,  $r > g$  is the condition that needs to obtain before each individual has communicative access to each other individual. By extension, this is the condition that needs to obtain before individual choices, strategies, and biases about who to connect

to and communicate with can fully account for network formation. Our simulations quantify what happens when this condition does not obtain (when  $0 < r < g$ ), and when therefore spatial constraints play a role in network formation. An interesting direction for future work, in models and experiments, would be to combine individual connection biases with spatial constraints.

One mechanism that starts to play a role in network formation when  $r < g$  is mobility. In their paper reporting a similar model, Vining and colleagues discuss a distinction between solid and liquid brains [35]. Solid brains, such as human brains and computer chips, have elements and links in more or less fixed positions, whereas liquid brains, such as swarms and slime moulds, consist of mobile elements that form transient links [41]. Vining and colleagues note that in liquid brains, mobility can play the role that physical links can play otherwise: connecting nodes, creating a pathway enabling information sharing. This is what we see in our simulations when  $r > g$ : because agents are situated in an environment and communication is range-constrained, moving through that environment becomes a mechanism for network formation. As  $r : g$  decreases, mobility becomes the dominant mechanism for connection; as  $r : g$  increases, links take over. Additionally, as population density increases, node properties becomes increasingly global and determined by  $r$  as the coordinate space becomes saturated and mobility becomes impossible. As the mobility mechanism disappears, models of networks on fixed lattices may therefore become more applicable under these circumstances.

Real individuals will of course show more intelligent mobility patterns than random movement. Moreover, random movement can be implemented in ways different from our model. A more standard implementation of movement direction in agent-based models is for agents to select from a uniform distribution of angles rather than directly from integer coordinate 'tiles.' In a recent paper, Chimento and Farine simulated this implementation of random movement as well as movement patterns where the distribution of angles was more concentrated towards specific directions, and where agents move towards resources in the environment [34]. Using data from cell phone towers, researchers have found that human displacements over time are approximated by agents selecting from a power-law

distribution of distances. Most of us move small to no distances most of the time, and greater distances some of the time; in addition, a small number of people travels much greater distances [42, 43]. One direction for future work is to combine our results of varying range and population size with these more realistic mobility patterns, and to test the fit of different mobility patterns to observational data of human communication networks, employing our model to see the role of spatial constraints to communication in the real world.

Apart from mobility, as discussed, we found a role for population size and density in the formation of communication networks. The role of population size in transmission processes has been discussed in literature on models in cultural evolution. Models have demonstrated that greater population size, under the right demographic and network connectivity circumstances, increases a population's ability to create and maintain complex skills [8, 44, 45, 46]. Our simulations show a different role for population size: increasing  $N$  in a bounded space increases population density, increasing the probability for randomly moving agents to encounter each other, creating denser networks for communication. Under the spatial constraints of a bounded environment and limited-range communication, population size influences not just transmission, but the communication network infrastructure that makes transmission possible.

One limitation of the present work is that though we quantify the impact of a bounded environment, the space itself is empty and unobstructed. The structure of real environments might significantly impact the possibilities of communication, introducing more complexity as well as realism into the spatial computation of network structure. A second limitation is that we consider only single-layer networks with global values for communication range, while real communicating systems may use different and overlapping communication media and technologies with different effective ranges. A third limitation is that we compare the ranged model to only one type of non-spatial model. Comparison to (dynamic versions of) other 'standard' non-spatial network generation algorithms such as small-world and connected-caveman graphs [36, 47] would paint a broader picture of the impact of including spatial constraints in network generation

algorithms. All three of these limitations would be fruitful directions for future work.

Leaving the role of spatial constraints out of the picture (for example, by over-relying on digital communication data, experimental settings where participants are all in the same space, or traditional network generation algorithms) could lead one to suggest that the mechanisms driving human communication network formation are primarily in psychology and behavior. However, including them in a model shows that, compared to a non-spatial model, these constraints alone can have a major impact on our predictions of network structure. One advantage of physical properties such as location and communication range as an explanatory mechanism of real communication networks is that they are much more straightforward to interpret, test and implement than hypotheses about drivers of human psychology and behavior. The simulations reported in this paper provide tools to understand communication networks as the product of a process of collective computation which does not just include choices by isolated individuals but also their surrounding environment.

## References

1. Cowgill B, Wolfers J, Zitzewitz E. Using Prediction Markets to Track Information Flows: Evidence from Google. In: Das S, Ostrovsky M, Pennock D, Szymanski B, editors. Auctions, Market Mechanisms and Their Applications. vol. 14. Berlin, Heidelberg: Springer Berlin Heidelberg; 2009. p. 3–3.
2. Stopczynski A, Pentland AS, Lehmann S. How Physical Proximity Shapes Complex Social Networks. *Scientific Reports*. 2018 Dec;8(1):17722.
3. Tóth G, Wachs J, Di Clemente R, Jakobi Á, Ságvári B, Kertész J, et al. Inequality Is Rising Where Social Network Segregation Interacts with Urban Topology. *Nature Communications*. 2021 Feb;12(1):1143.
4. Momennejad I. Collective Minds: Social Network Topology Shapes Collective

- Cognition. *Philosophical Transactions of the Royal Society B: Biological Sciences*. 2021 Dec;377(1843):20200315.
5. Centola D. The Network Science of Collective Intelligence. *Trends in Cognitive Sciences*. 2022 Nov;26(11):923–941.
  6. Centola D. The Spread of Behavior in an Online Social Network Experiment. *Science*. 2010 Sep;329(5996):1194–1197.
  7. Centola D, Baronchelli A. The Spontaneous Emergence of Conventions: An Experimental Study of Cultural Evolution. *Proceedings of the National Academy of Sciences of the United States of America*. 2015 Feb;112(7):1989–1994.
  8. Moser C, Smaldino PE. Innovation-Facilitating Networks Create Inequality. *Proceedings of the Royal Society B: Biological Sciences*. 2023;290(2003):20230672.
  9. Derex M, Boyd R. Partial Connectivity Increases Cultural Accumulation within Groups. *Proceedings of the National Academy of Sciences*. 2016 Mar;113(11):2982–2987.
  10. Derex M, Perreault C, Boyd R. Divide and Conquer: Intermediate Levels of Population Fragmentation Maximize Cultural Accumulation. *Philosophical Transactions of the Royal Society B: Biological Sciences*. 2018 Feb;373(1743):20170062.
  11. Lazer D, Friedman A. The Network Structure of Exploration and Exploitation. *Administrative Science Quarterly*. 2007 Dec;52(4):667–694.
  12. Bavelas A. Communication Patterns in Task-Oriented Groups. *The Journal of the Acoustical Society of America*. 1950 Nov;22(6):725–730.
  13. Conte A, Di Cagno D, Sciubba E. Strategies in Social Network Formation. *Theory and Decision*. 2009;67(2):161–193.
  14. Almaatouq A, Noriega-Campero A, Alotaibi A, Krafft PM, Moussaid M, Pentland A. Adaptive Social Networks Promote the Wisdom of Crowds. *Proceedings*

- of the National Academy of Sciences of the United States of America. 2020 May;117(21):11379–11386.
15. Nakayama S, Krasner E, Zino L, Porfiri M. Social Information and Spontaneous Emergence of Leaders in Human Groups. *Journal of the Royal Society Interface*. 2019 Feb;16(151).
  16. Kendal RL, Boogert NJ, Rendell L, Laland KN, Webster M, Jones PL. Social Learning Strategies: Bridge-Building between Fields. *Trends in Cognitive Sciences*. 2018 Jul;22(7):651–665.
  17. Boyd R, Richerson PJ. *Culture and the Evolutionary Process*. Chicago, IL: University of Chicago Press; 1985.
  18. Laland KN. Social Learning Strategies. *Learning & Behavior*. 2004 Feb;32(1):4–14.
  19. Canteloup C, Hoppitt W, van de Waal E. Wild Primates Copy Higher-Ranked Individuals in a Social Transmission Experiment. *Nature Communications*. 2020 Jan;11(1):459.
  20. Kendal R, Hopper LM, Whiten A, Brosnan SF, Lambeth SP, Schapiro SJ, et al. Chimpanzees Copy Dominant and Knowledgeable Individuals: Implications for Cultural Diversity. *Evolution and Human Behavior*. 2015 Jan;36(1):65–72.
  21. Smith JE, Natterson-Horowitz B, Alfaro ME. The Nature of Privilege: Intergenerational Wealth in Animal Societies. *Behavioral Ecology*. 2022 Feb;33(1):1–6.
  22. Mulder MB, Bowles S, Hertz T, Bell A, Beise J, Clark G, et al. Intergenerational Wealth Transmission and the Dynamics of Inequality in Small-Scale Societies. *Science*. 2009 Oct;326(5953):682–688.
  23. Cantor M, Whitehead H. The Interplay between Social Networks and Culture: Theoretically and among Whales and Dolphins. *Philosophical Transactions of the Royal Society B: Biological Sciences*. 2013 May;368(1618):20120340.

24. Ilany A, Holekamp KE, Akçay E. Rank-Dependent Social Inheritance Determines Social Network Structure in Spotted Hyenas. *Science* (New York, NY). 2021 Jul;373(6552):348–352.
25. Bokányi E, Heemskerk EM, Takes FW. The Anatomy of a Population-Scale Social Network. *Scientific Reports*. 2023 Jun;13(1):9209.
26. Piketty T. About *Capital in the Twenty-First Century*. *American Economic Review*. 2015 May;105(5):48–53.
27. Gemar A. Parental Status Connection and Social Network Variety in Adulthood. *Societies*. 2024 Feb;14:26.
28. Langbauer WR. Elephant Communication. *Zoo Biology*. 2000;19(5):425–445.
29. Kota M, Olzer R. Insect Communication. In: Vonk J, Shackelford TK, editors. *Encyclopedia of Animal Cognition and Behavior*; 2022. p. 3465–3471.
30. Acerbi A. *Cultural Evolution in the Digital Age*. Cambridge, MA: MIT Press; 2020. Available from: <https://mitpress.mit.edu/9780262044712/cultural-evolution-in-the-digital-age/>.
31. Backstrom L, Boldi P, Rosa M, Ugander J, Vigna S. The anatomy of the Facebook social graph. In: *Proceedings of the 21st international conference on World Wide Web*. ACM; 2011. p. 831–840.
32. Onnela JP, Saramäki J, Hyvönen J, Szabó G, Lazer D, Kaski K, et al. Structure and Tie Strengths in Mobile Communication Networks. *Proceedings of the National Academy of Sciences of the United States of America*. 2007 Jun;104:7332–6.
33. Bokányi E, Novák M, Jakobi Á, Lengyel B. Urban Hierarchy and Spatial Diffusion over the Innovation Life Cycle. *Royal Society Open Science*. 2022 May;9(5):211038.
34. Chimento M, Farine DR. The Contribution of Movement to Social Network Structure and Spreading Dynamics under Simple and Complex Transmission.

- Philosophical Transactions of the Royal Society B: Biological Sciences. 2024 Oct;379(1912):20220524.
35. Vining WF, Esponda F, Moses ME, Forrest S. How Does Mobility Help Distributed Systems Compute? *Philosophical Transactions of the Royal Society B: Biological Sciences*. 2019 Jun;374(1774):20180375.
  36. Watts DJ, Strogatz SH. Collective Dynamics of ‘Small-World’ Networks. *Nature*. 1998 Jun;393(6684):440–442.
  37. Humphries MD, Gurney K. Network ‘Small-World-Ness’: A Quantitative Method for Determining Canonical Network Equivalence. *PLoS ONE*. 2008 Apr;3(4):e0002051.
  38. Erdős P, Rényi A. On random graphs. *Publicationes Mathematicae Debrecen*. 1959;6:290–297.
  39. Newman MEJ. The structure and function of complex networks. *SIAM Review*. 2003;45(2):167–256.
  40. Barabási AL, Albert R, Jeong H. Scale-free characteristics of random networks: the topology of the world-wide web. *Physica A: Statistical Mechanics and its Applications*. 2000;281(1-4):69–77.
  41. Solé R, Moses M, Forrest S. Liquid Brains, Solid Brains. *Philosophical Transactions of the Royal Society B: Biological Sciences*. 2019 Apr;374(1774):20190040.
  42. Gonzalez MC, Hidalgo C, Barabasi AL. Understanding Individual Human Mobility Patterns. *Nature*. 2008 Jul;453:779–82.
  43. Almaatouq A, Prieto-Castrillo F, Pentland A. Mobile Communication Signatures of Unemployment. In: Aiello LM, McFarland D, editors. *Computational Social Science: Discovery and Prediction*; 2016. p. 413–428.
  44. Baldini R. Revisiting the Effect of Population Size on Cumulative Cultural Evolution. *Journal of Cognition and Culture*. 2015;15(1-2):118–139.



45. Deffner D, Kandler A, Fogarty L. Effective Population Size for Culturally Evolving Traits. *bioRxiv*. 2021 Sep;.
46. Henrich J. Demography and Cultural Evolution: How Adaptive Cultural Processes Can Produce Maladaptive Losses—The Tasmanian Case. *American Antiquity*. 2004 Apr;69(2):197–214.
47. Watts DJ. Networks, dynamics, and the small-world phenomenon. *American Journal of Sociology*. 1999;105(2):493–527.